



# TECHNICAL NOTE

D-2007

## MEASUREMENT OF TORSIONAL RIGIDITY OF STIFFENED PLATES

By Herbert Becker and George Gerard

Prepared under Grant No. NsG-17-59 by  
NEW YORK UNIVERSITY  
for

NATIONAL AERONAUTICS AND SPACE ADMINISTRATION  
WASHINGTON

July 1963



TECHNICAL NOTE D-2007

MEASUREMENT OF TORSIONAL RIGIDITY OF STIFFENED PLATES

By Herbert Becker and George Gerard  
New York University

ABSTRACT

An instrument developed for measuring torsional rigidity of stiffened structures is described. Use of the instrument is discussed and calibration procedures are explained. Perspective on the investigation is provided by the inclusion of pertinent theories for torsional rigidity with which the experimental measurements are compared.

NATIONAL AERONAUTICS AND SPACE ADMINISTRATION



## TABLE OF CONTENTS

|   | <u>Page</u> |
|---|-------------|
| INTRODUCTION  | 1           |
| TABLE OF SYMBOLS  | 4           |
| PRESENT STATUS OF EXPERIMENTAL DATA                               | 6           |
| TORSIONAL RIGIDITY THEORY   | 8           |
| EXPERIMENTAL DETERMINATION OF $J_i$                               | 14          |
| DESCRIPTION OF EXPERIMENTAL EQUIPMENT                             | 22          |
| EXPERIMENTAL ERRORS   | 27          |
| EXPERIMENTS   | 31          |
| <br>FIGURE  |             |
| 1 Plate Geometries  | 12          |
| 2 Schematic Test Set-up   | 15          |
| 3 Details of $\Delta\theta / \Delta x$                            | 17          |
| 4 Angular Deflection Measurement Circuit                          | 18          |
| 5 Typical Test Data Curves  | 20          |
| 6 Experimental Set-up   | 23          |
| 7 Individual Calibration Curves for the Four Capacitor<br>Sensors | 26          |
| 8 Torque vs Twist for Flat and Ribbed Plates of Table I           | 33          |
| <br>TABLE   |             |
| I Summary of Experimental Data                                    | 34          |



NATIONAL AERONAUTICS AND SPACE ADMINISTRATION

---

TECHNICAL NOTE D-2007

---

MEASUREMENT OF TORSIONAL RIGIDITY OF STIFFENED PLATES

By Herbert Becker and George Gerard

INTRODUCTION

General Background

As the result of a need for data on the torsional rigidity of the wall of an orthotropic shell, this program of development of an instrument to measure that quantity was initiated. Although a prime need for torsional rigidity data occurs in connection with instability problems, the information is of value in any branch of shell analysis. This is accentuated by the meager experimental data reported to date, and the fact that close agreement of these data with theory is lacking.

This situation is emphasized in analysis of instability of stiffened construction since investigations have revealed that use of incorrect values for torsional rigidity may lead to large inaccuracies in prediction of load carrying capacity, an extreme case being general instability of stiffened shells loaded in axial compression or in bending. Becker presented a detailed discussion of this case in Reference 1.

Orthotropic shell stress analysis also is constrained by the lack of experimental background. During investigations in the

present program it became increasingly difficult to formulate an accurate description of orthotropic behavior since the commonly accepted definition of close stiffener spacing did not appear to apply to torsional rigidity although it seemed to be satisfactory for bending rigidity. Because of this fact, use of the term "orthotropic" is avoided in this report in connection with stiffened construction. A detailed discussion of orthotropicity and the behavior of stiffened plate construction was furnished by Gerard and Becker in Part VII of the Handbook of Structural Stability (Reference 2), which contains background for the present program since the work described in this report was confined to flat plates.

#### Status of Rigidity Determination

In stiffened plate theory the bending and twisting moments are related to the plate curvatures through the stiffnesses. If Poisson's ratio is chosen equal to zero, as was done by Becker and Gerard in developing the stability theory for orthotropic shells, (Reference 3), then  $M_x = EI_x (\partial^2 w / \partial x^2)$ ,  $M_y = EI_y (\partial^2 w / \partial y^2)$  and  $M_{xy} = 1/2 GJ (\partial^2 w / \partial x \partial y)$  where  $EI_x$ ,  $EI_y$  and  $GJ$  are the x and y bending rigidities and the torsional rigidity respectively.

Theories exist for calculating these rigidities. However, in general only the predicted bending rigidities have been successfully substantiated experimentally. As is discussed below, there is generally



poor agreement between theory and experiment for determining GJ, part of which appears to be due to the type of equipment used to measure this quantity. The program which was initiated to develop equipment designed to measure GJ accurately on a stiffened plate is described in this report.

### Organization of Report

The principal purpose of this report is to provide a detailed description of the instrument which was developed to measure torsional rigidity of stiffened construction, to describe its use, and to compare data obtained with the instrument to the predictions of theory. The present phase of the program was confined to flat plates. Such data should apply with reasonable accuracy to thin shells as well.

To provide perspective for the program, the present state of information on experimental data precedes the main report, which contains pertinent theories for torsional rigidity with which experimental data are compared.

### Acknowledgment

The experiments for this investigation were performed by Messrs. Robert Winter and Louis Amelio who also contributed to the development of the experimental equipment.

## TABLE OF SYMBOLS

|            |   |
|------------|---|
| a          | length of plate, in.  |
| b          | width of plate, in.   |
| $b_s$      | width of repeating section of plate, in.  |
| d          | diameter of largest circle inscribed in rib sheet intersection, in.                     |
| E          | modulus of elasticity, psi.   |
| G          | shear modulus of elasticity, $E/[2(1+\nu)]$ , psi.                                      |
| $J_x, J_y$ | torsional moments of inertia in x and y directions, in. <sup>4</sup>                    |
| $J_1$      | torsional moment of inertia in any principal direction, in. <sup>4</sup>                |
| $J_o$      | nominal torsional moment of inertia, $bt^3/3$ , in. <sup>4</sup>                        |
| L          | gauge length of specimen, in.   |
| m          | slope of the $\Sigma_{cal}$ vs $\theta_{cal}$ curve, volts/radian                       |
| n          | slope of the $\Sigma_{test}$ vs T curve, volts/in-lb.                                   |
| r          | fillet radius at rib-sheet intersection, in.  |
| T          | Torque applied to plate, in-lb.   |
| t          | thickness of plate, in.   |
| x,y        | orthogonal coordinates in plane of plate, corresponding to principal axes of plate, in. |
| $\alpha$   | coefficient   |
| $\beta$    | coefficient   |
| $\nabla^2$ | differential operator, $\partial^2/\partial x^2 + \partial^2/\partial y^2$              |
| $\theta$   | angular deflection of plate, radians  |

## TABLE OF SYMBOLS

(Continued)

|          |   |
|----------|---|
| $\nu$    | Poisson's ratio   |
| $\Sigma$ | electrical system response to angular deflection, volts |
| $\sigma$ | axial stress, psi.                                      |
| $\tau$   | shear stress, psi.                                      |
| $\phi$   | warping function  |

### Subscripts

|     |  |
|-----|--|
| A,B | stations of measurement along axis of specimen |
| cal | calibration                                    |
| r   | rib  |
| s   | sheet  |

## PRESENT STATUS OF EXPERIMENTAL DATA

Libove and Hubka (Reference 4) investigated elastic constants for corrugated core sandwich plates. A theoretical determination of torsional rigidity was made for a 3/4 inch thick plate, together with an experimental check. The test result was 2.8 percent higher than theory. Torque was applied to the plate through equal and opposite forces perpendicular to the plate at the four corners. Stiff side frame members transmitted the corner loads into the plate as running shear. Twist was measured by differential transverse motion.

Dow, Libove and Hubka (Reference 5) determined elastic constants for waffle plates both theoretically and experimentally. Six tests were performed as in Reference 4 on plates with the stiffening system at various angles to the plate edges. The band representing the range of torsional rigidity between the theoretical upper and lower limits is approached most closely for the 45 degree stiffened plates. The data for plates with stiffeners at other angles lie either above or below the theory band. The average of these tests departs from the center of the theory band by about 50 percent.

Dow, Libove and Hubka, in this same investigation, tested four plates with 45 degree stiffening. In this case the theory band was essentially a single curve. The experimental data averaged approximately 80 percent of the theoretical value with one test approaching

to within 85 percent of theory.

Crawford and Libove (Reference 6) mentioned additional tests but reported no specific data.

Hoppmann (Reference 7) tested three square plates with ribbing in one direction only. The plates were loaded transversely at the four corners but no side stiffening plates were used. However, the experimental data were not compared to theory. Hoppmann, Huffington and Magness (Reference 8) tested two plates of the same character. The tests, in which strain gages were used to determine torsional rigidity, were compared with theoretical predictions. The experimental value was 1 percent high for one plate and 13 percent low for the other. In these two plates the rib material constituted a relatively small percentage of the total cross section.

The status of experimental data on torsional rigidity, therefore, consists of one test on a corrugated core sandwich plate in good agreement with theory, six tests on waffle plates with a deviation from theory of about 50 percent, four tests on 45 degree waffle plates with a deviation from theory of approximately 20 percent, and two tests on unidirectionally stiffened plates in fair agreement with theory. No experimental data are available on isotropic plates, or upon the effect of curvature on torsional rigidity. It is also noteworthy that existing data pertain to relatively stiff structures. Thin sheet tests have not been reported.

## TORSIONAL RIGIDITY THEORY

### Introduction

In Taylor's mathematical theory (Reference 3) which depicts the behavior of a stiffened cylinder, the torsional rigidity appears as the sum of two terms,  $J_x$  and  $J_y$ . This separation arises from the assumption that the stiffeners are linear elements. In a circular cylindrical shell with longitudinal and circumferential stiffening the effective torsional rigidity would appear in the differential equation. That is,  $J = J_s + J_f$  using the notation in the report by Becker and Gerard on orthotropic shells (Reference 3).

The plates which have been investigated experimentally in this present program were stiffened in no more than one direction, which could apply to either the frames or longitudinals of a shell. In order to indicate this general applicability the torsional rigidity of each specimen in this report has been designated  $J_i$  where the specific value of  $i$  would depend upon the application of the data in subsequent investigations. The quantity,  $J_i$ , is the torsional rigidity of the structure with the units in.<sup>4</sup>

Theoretical approaches to the determination of  $J_1$  have been reported by Crawford and Libove (Reference 6), Timoshenko (Reference 9), and by Lyse and Johnston (Reference 10). As in the case of experimental data, existing theory for determination of  $J_1$  is confined to flat plates.

### General Theory

The mathematical theory of torsion in a long structural element of constant cross section is well known and has been treated extensively in the literature on elasticity (Reference 9, for example). Essentially the problem is to find a warping function,  $\phi$ , subject to the conditions

$$\nabla^2 \phi + 2G\theta = 0 \quad (1)$$

$$\tau_{xz} = \partial\phi/\partial y, \quad \tau_{yz} = -\partial\phi/\partial x \quad (2)$$

$$\sigma_x = \sigma_y = \sigma_z = \tau_{xy} = \partial\tau_{xz}/\partial z = \partial\tau_{yz}/\partial z = \partial\tau_{xz}/\partial x + \partial\tau_{yz}/\partial y = 0 \quad (3)$$

Solutions to Eq.(1) have been found analytically for some special cases and by the membrane analogy (Trayer and March, Reference 11) for shapes which are not amenable to closed form mathematical solutions.

The structures of particular interest in the present investigation are plates with proportions in the ranges  $5 < b/t < 100$  and  $3 < a/b < 10$ . The isotropic limiting case has a rectangular cross section. More general plates are ribbed uniformly across the width (Fig. 1) with cross sections which are constant along the length. As discussed in the Introduction, the term "orthotropic" has been avoided when referring to these plates. Specific theoretical results which apply to these types of plates are presented in the following sections.

### Isotropic Plate Theory

As demonstrated by Timoshenko (Reference 9), the solution to Eq.(1) for rectangular plates yields

$$d\theta/dx = T/J_1 G \quad (4)$$

$$J_1 = (bt^3/3)[1 - 0.6274t/b \sum_{n=1,3,5,\dots}^{\infty} (1/n^5) \tanh(n\pi b/2t)] \quad (5)$$

For the range of proportions defined above,

$$J_1 = (bt^3/3)[1 - 0.630(t/b)]$$

It is convenient to refer to  $bt^3/3$  as  $J_0$ . Therefore,

$$J_1/J_0 = 1 - 0.630(t/b) \quad (6)$$

When  $5 < b/t < 100$ , then  $0.874 < J_1/J_0 < 0.994$ .



For a detailed analysis of this problem Reference 9 may be consulted.

### Ribbed Plate Theory

The computation of  $J_1$  for a ribbed plate was developed by Lyse and Johnston (Reference 10) in a semiempirical form utilizing results from the membrane analogy. The general calculation form essentially considers a ribbed plate to be a group of rectangular plates with corrections to be made for the effects of finite plate widths and the intersection radii at the rib-plate joints.

The expression used in this report for  $J_1$  is

$$J_1 = \Sigma [b_s t_s^3 / 3 + (1 + 3k) b_r t_r^3 / 6 + \alpha d^4] - 0.210 t_s^3 \quad (7)$$

as provided by combining the results of Lyse and Johnston with those of Timoshenko for a finite width ribbed plate with a typical section as shown in Fig. 1. The second term in the summation appears after applying Eq.(5) to the rib, where

$$k = (1/3) [1 - 0.6274 (t_r / b_r) \sum_{n=1,3,5,\dots}^{\infty} (1/n^5) \tanh(n\pi b_r / 2t_r)] \quad (8)$$

The value of  $k$  has a maximum limit of  $1/3$ , effectively reached when  $b_r / t_r \geq 100$ . The term  $\alpha d^4$  is the contribution of the intersection of the sheet with the rib. The dimension  $d$ , the diameter of the largest circle to be inscribed in the intersection (Fig. 1), may be expressed analytically as

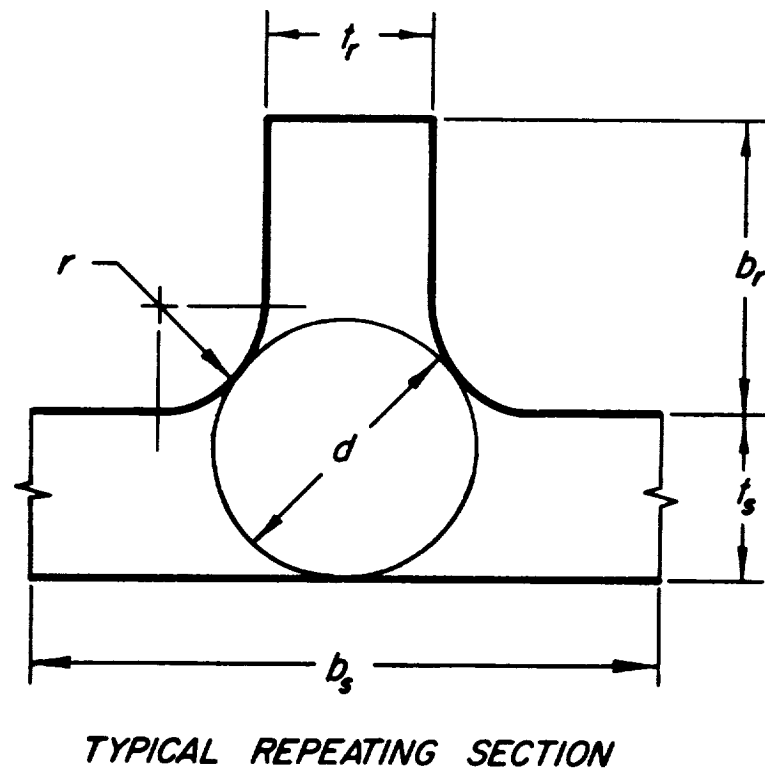
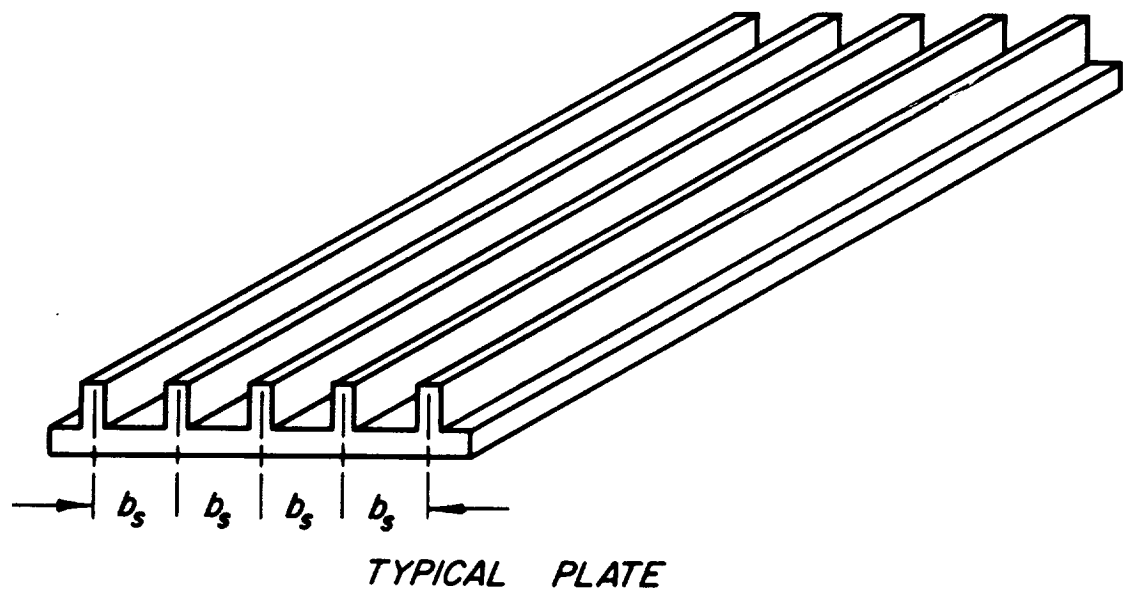


FIGURE 1 PLATE GEOMETRIES.

$$d = [(r + t_s)^2 + t_r(r + t_r/4)]/(2r + t_s) \quad (9)$$

Also

$$\alpha = 0.094 + 0.070r/t_s \quad (10)$$

as given in Reference 10. The summation extends over all repeated rib-plate intersections. Eq.(7) reduces to Eq.(6) in the isotropic limit in which case  $b_r = d = 0$ .

Crawford and Libove recommended that Eq.(7) be used only when  $r/t_s \leq 1$  and  $t_r/t_s \leq 2$ .

## EXPERIMENTAL DETERMINATION OF $J_1$

### Principle

Before proceeding with a detailed description of the testing machine, it is pertinent at this point to describe the experimental principle involved to aid in understanding the construction details of the machine. The experimental determination of  $J_1$  was accomplished by utilization of the torque-twist relation for a bar,

$$J_1 = \frac{T}{G(\Delta\theta/\Delta x)} \quad (11)$$

Rotations and torques were measured in the torsion testing machine and  $G$  was obtained from material property data for  $E$  and  $\nu$  through the relation  $E = 2(1+\nu)G$ .

Torque was applied to each test specimen by means of dead weights eccentric to the testing machine axle (Fig. 2) and consequently was determinable with little effort. However, measurement of  $\Delta\theta/\Delta x$  required a slightly more complex procedure, described in the following section.

### Measurement of $\Delta\theta/\Delta x$

The twist rate,  $\Delta\theta/\Delta x$ , was obtained by measuring rotation

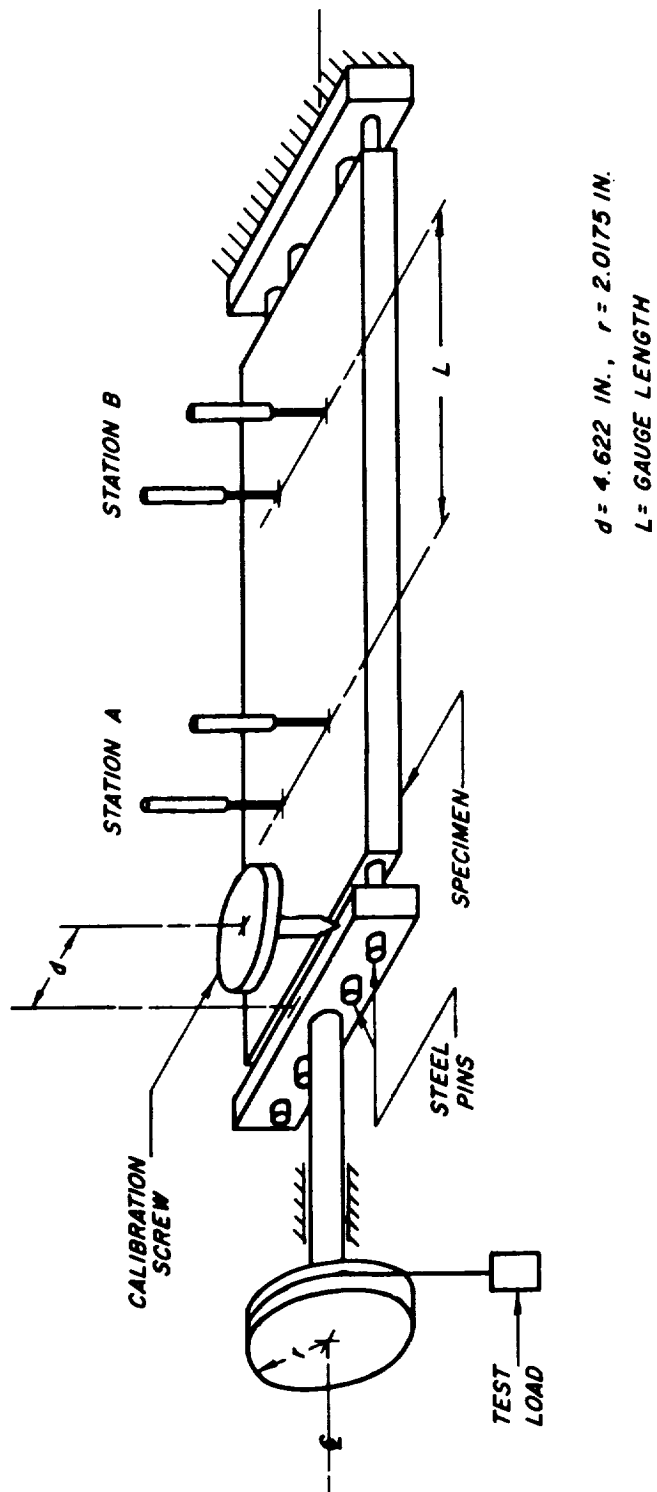


FIGURE 2 SCHEMATIC TEST SET-UP.

of a specimen at two stations along the twist axis. Referring to Fig. 3,

$$\Delta\theta/\Delta x = (\theta_A - \theta_B)/L \quad (12)$$

where L is the axial distance between stations A and B. The twist at each station was obtained by a calibrated pair of differential capacitor sensors developed by Papirno, Reference 12. These sensed the motion of the specimen surface perpendicular to the twist axes at a pair of points equidistant from the twist axis (Figs. 3 and 4).

The calibration procedure consisted of applying a rigid body rotation to the specimen while it was in the testing machine, simultaneously recording sensor signal and specimen rotation. In all cases a rotation range of roughly 6 degrees was found in which the twist-signal curve was essentially linear. Care was taken during the running of each  $J_I$  measurement to maintain  $\theta_A$  and  $\theta_B$  within this range to permit utilizing the data reduction process described below. A typical set of calibration curves is shown in Fig. 5a, for both stations A and B.

The spacing of a sensor pair astride the rotation axis is variable depending upon the character of test specimen, as is also the case with the spacing between stations A and B. This distance, L, is recorded for each test. The sensor pair spacing is absorbed in the calibration signal output.

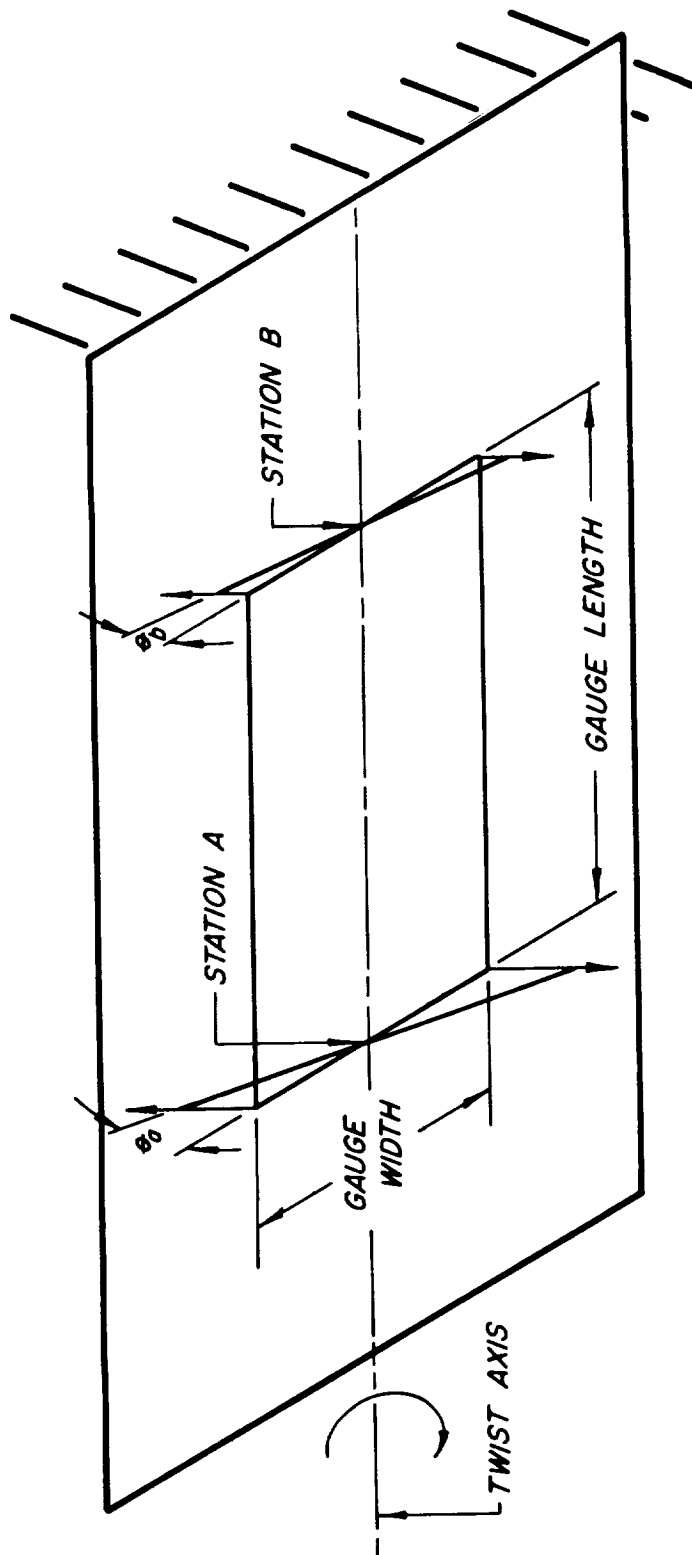


FIGURE 3 DETAILS OF  $\Delta\theta/\Delta x$ .

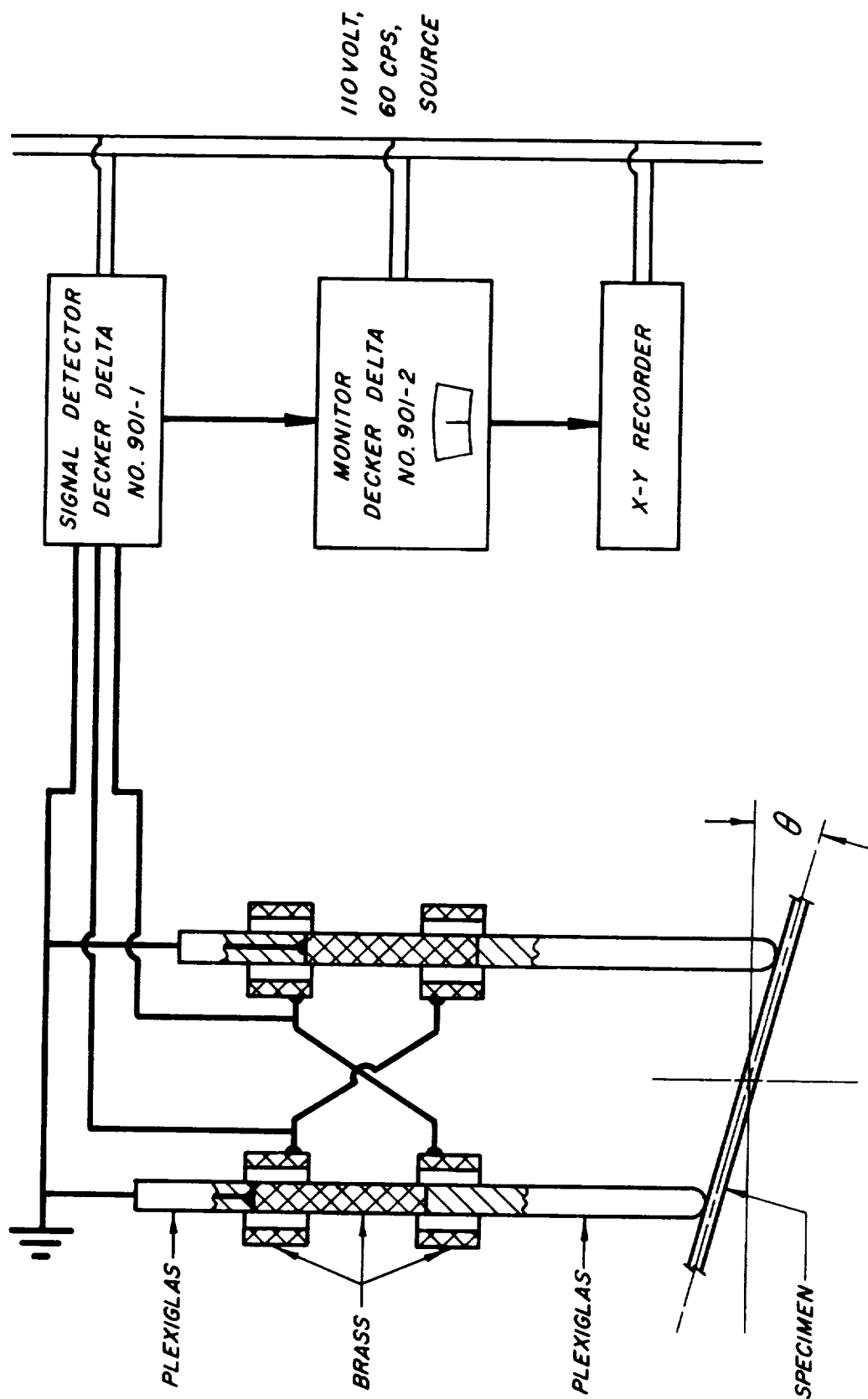


FIGURE 4 ANGULAR DEFLECTION MEASUREMENT CIRCUIT.



### Computation of $J_i$

A typical set of sensor data at a given station consists of a curve relating  $\Sigma_{cal}$  to  $\theta_{cal}$  and a curve relating  $\Sigma_{test}$  to  $T$ , as shown in Fig. 5. If these curves are straight lines of slopes  $m$  and  $n$  respectively, then

$$\frac{\Delta \Sigma_{cal}}{\Delta \theta_{cal}} = \frac{\Delta \Sigma_{test}}{\Delta \theta_{test}} = m, \quad \frac{\Delta \Sigma_{test}}{\Delta T} = n \quad (13)$$

Consequently,

$$\frac{\Delta \theta_{test}}{\Delta T} = \frac{n}{m} \quad (14)$$

or

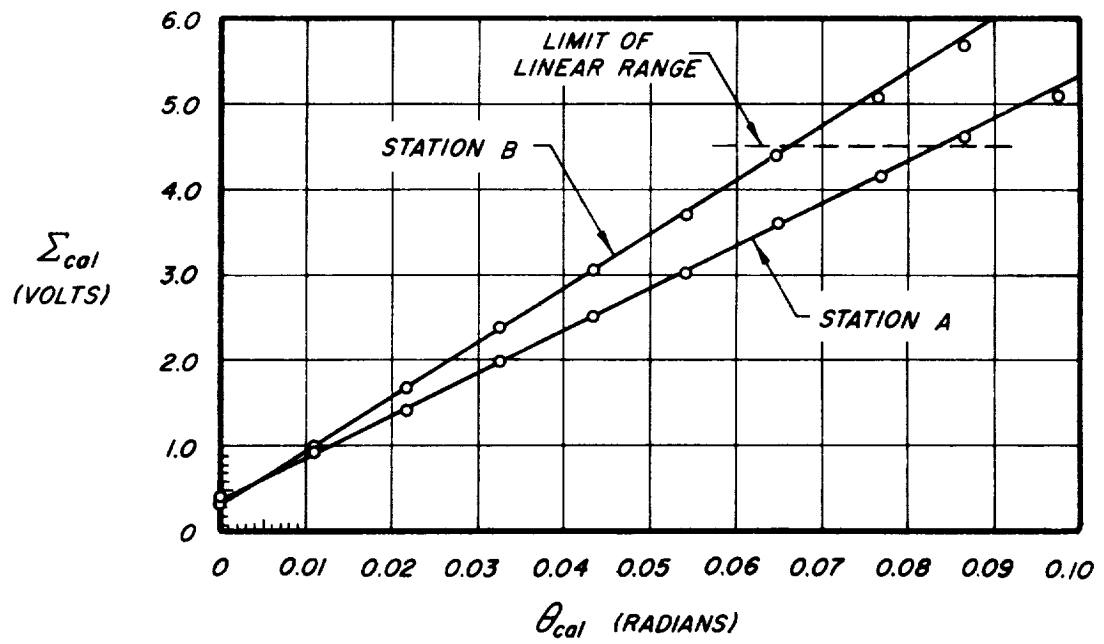
$$\left( \frac{\Delta \theta_{test}}{\Delta T} \right)_A = \left( \frac{n}{m} \right)_A \quad (15)$$

$$\left( \frac{\Delta \theta_{test}}{\Delta T} \right)_B = \left( \frac{n}{m} \right)_B \quad (16)$$

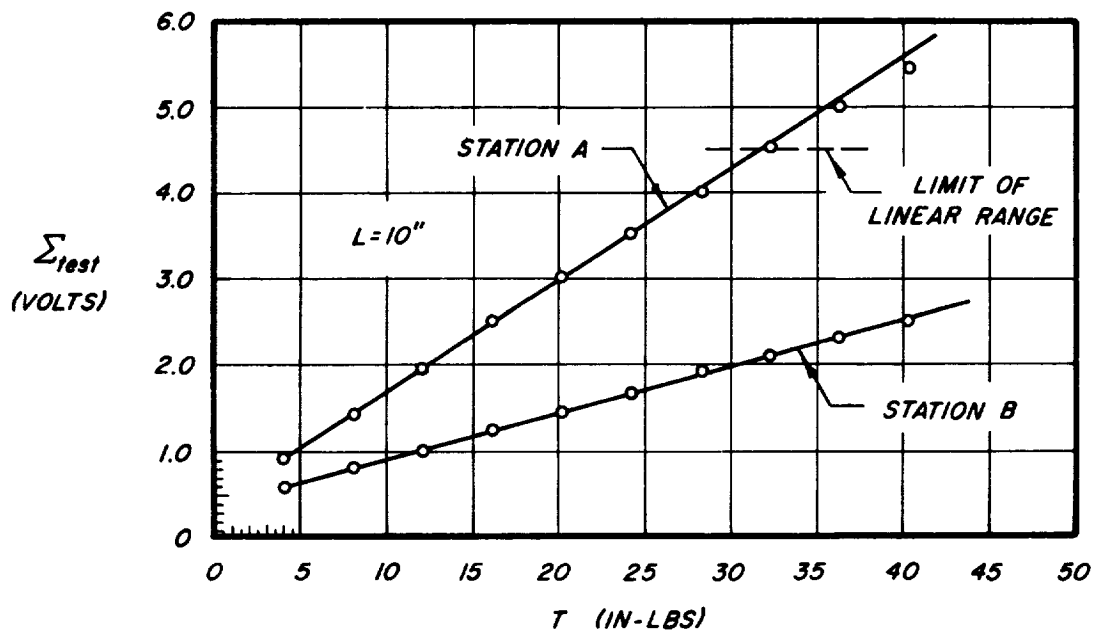
It follows, then, that

$$(\Delta \theta_{test})_A = (n/m)_A \Delta T \quad (17)$$

$$(\Delta \theta_{test})_B = (n/m)_B \Delta T \quad (18)$$



(a) CALIBRATION



(b) TEST RUN

FIGURE 5 TYPICAL TEST DATA CURVES.

and therefore in Eq.(11)  $\Delta\theta/\Delta x$  for a given T is replaced by  $\Delta(\Delta\theta)/\Delta x$  for a given  $\Delta T$ . That is,

$$J_1 = \frac{L\Delta T}{G[\Delta\theta_A - \Delta\theta_B]} \quad (19)$$

or, using Eqs.(17) and (18)

$$J_1 = \frac{L}{G[(n/m)_A - (n/m)_B]} \quad (20)$$

The units of  $n/m$  are radian/in-lb and consequently  $J_1$  will have the units of  $T/[G(\Delta\theta/\Delta x)]$  as in Eq.(11).

Because of the calibration procedure, utilization of Eq.(20) to determine  $J_1$  is simpler than plotting  $\Delta\theta/\Delta x$  as a function of T and employing Eq.(11). Furthermore, in the latter case, it would be necessary to transform from the  $\Delta T - \Delta\Sigma$  curve to the  $\Delta\theta - \Delta\Sigma$  curve thereby leading to errors in crossplotting. Such errors do not occur when using Eq.(20).

## DESCRIPTION OF EXPERIMENTAL EQUIPMENT

### Introduction

This section contains a detailed description of the equipment for applying torsion load and measuring twist during a test to determine  $J_1$ . A photograph of the equipment appears in Fig. 6, while Fig. 4 contains a circuit diagram for the capacitor twist measuring system.

Details of the equipment together with the calibration procedure and pertinent constants are included in the following paragraphs.

### General Description of Loading Machine

Torque is applied to the plate models in the device shown in Fig. 6. This is essentially a horizontal four column testing machine designed principally to induce twisting in a strip at the loading end with zero rotational motion at the support end. The sensor heads are mounted in pairs on cross bars clamped to the upper pair of columns. The rotation calibration screw is mounted on the front (or loading) plate with the screw tip pushing down upon the calibration crossbar.

The twisting trunnion lies in a ball bearing which is cleaned periodically to keep friction to a minimum. Measurements reveal that starting friction torque can be kept below 0.002 in-lb.

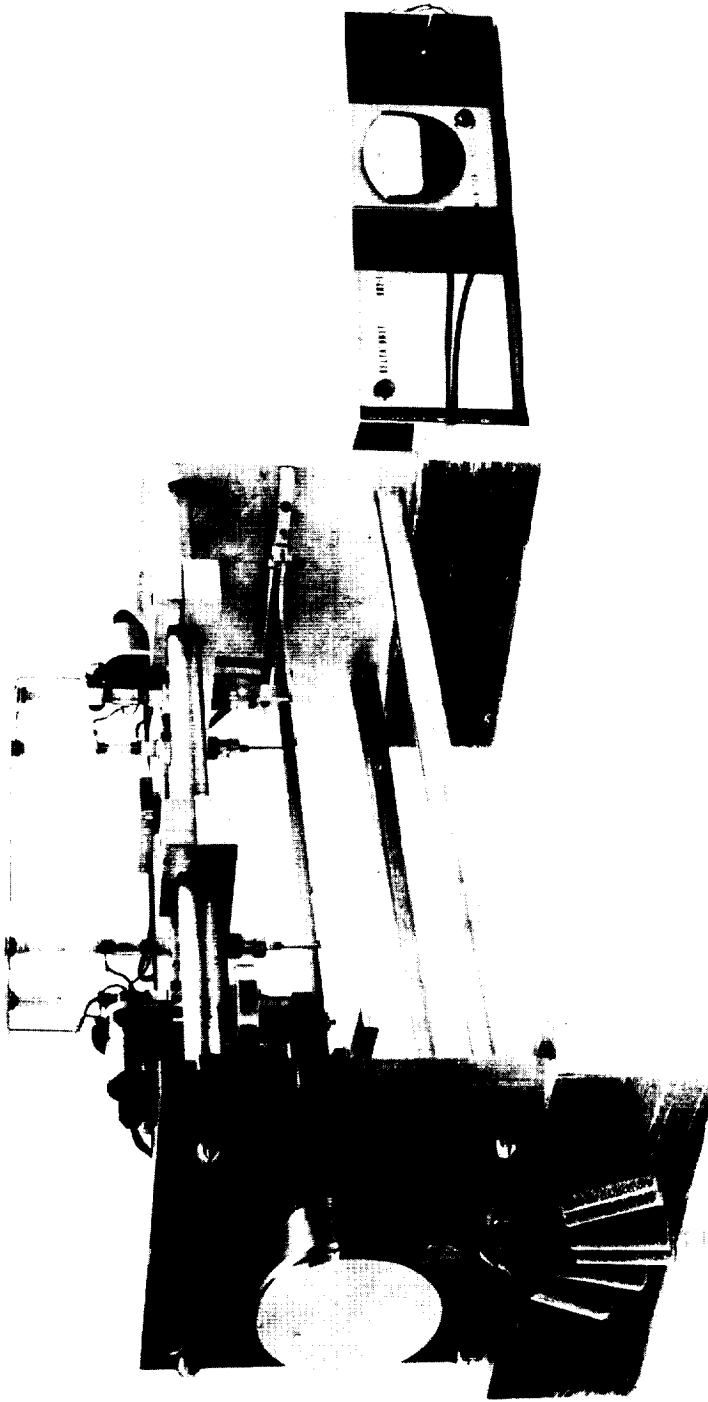


FIGURE 6 EXPERIMENTAL SET-UP.

Torque is applied through a pair of hard steel pins (Fig. 2) ground to minimize friction in order to avoid restraint of warping action.

#### Loading Machine Details

Dead weights are used to load the model by hanging them upon a thread in the groove of the loading head, the radius of which (including half the thread thickness) is 2.0175 in. Each weight consists of a plastic tube with lead shot which is weighed on a chemical balance to obtain loads as small as  $0.165 \pm 2 \times 10^{-5}$  lb. This permits application of dead load torque in minimum increments of 0.333 in-lb.

The calibration micrometer consists of a  $1/2$  - 80 thread with a 2.75 in. diameter disk on top marked off in 25 divisions. The lever arm to the loading trunnion axis is 4.622 in. Consequently, one division on the micrometer disk corresponds to a rotation of  $1.082 \times 10^{-4}$  radians, or  $6.199 \times 10^{-3}$  degrees. The micrometer disk can be interpolated easily to  $1/4$  of this value.

#### Twist Measuring System

As described previously, the twist is measured by differential normal motion over fixed lever arms utilizing capacitor sensors in pairs electrically connected so that the signal is proportional to the rotation of the calibration bar. A detailed discussion of the capacitor

design appears in the report by Papirno (Reference 12). The schematic electrical arrangement is shown in Fig. 4. The sensor pairs are shown in position in Fig. 6.

Each sensor was calibrated in place separately before pairing in order to bracket the linear range. Fig. 7 contains the calibration curves for all four sensors. After separate calibration the wiring was altered to obtain twist signals using the electrical arrangement shown in Fig. 4. The calibration curves varied slightly from day to day. Consequently, calibration was repeated immediately preceding each test.

Twist calibration was accomplished by applying selected twists and recording the corresponding voltages revealed by the dial on the Monitor 902-2. Voltage was plotted as ordinate against rotation as abscissa. A straight line was drawn through the data for best fit in the center of the linear range. The slope of this line yielded the value of  $m$ .

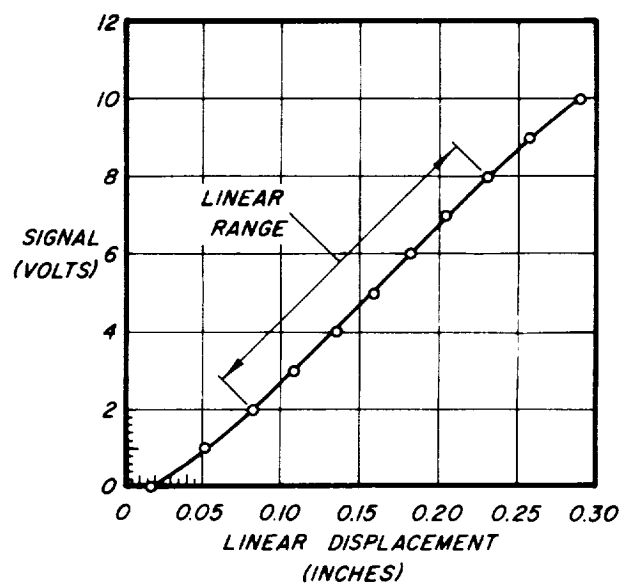
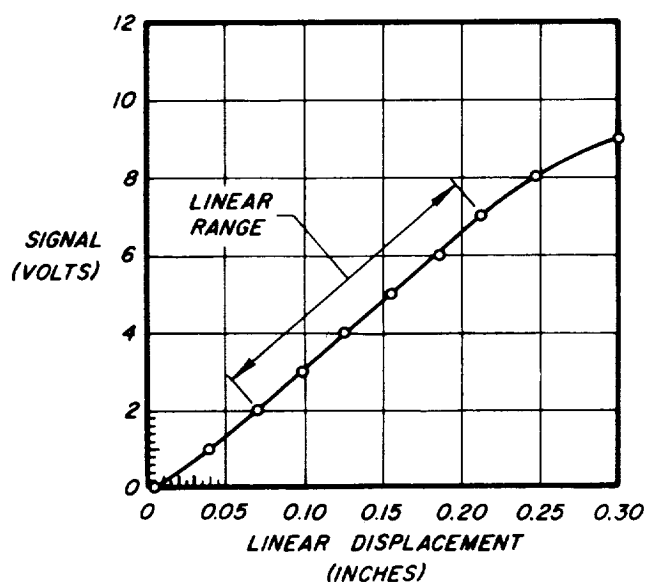
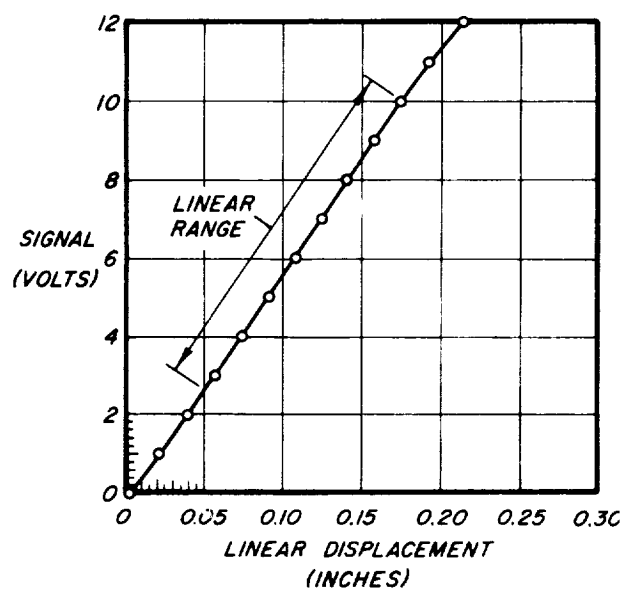
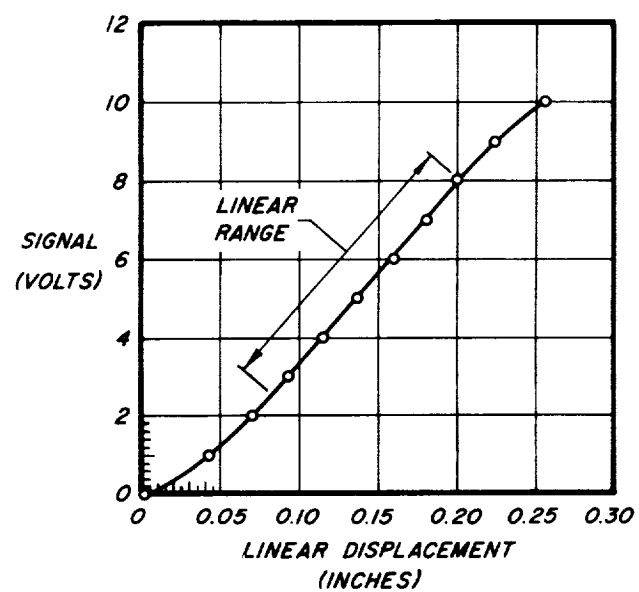


FIGURE 7 INDIVIDUAL CALIBRATION CURVES FOR THE FOUR CAPACITOR SENSORS.



## EXPERIMENTAL ERRORS

### Sources of Experimental Error

Experimental errors may be generated in the model, the loading system, the twist measuring system, and possibly in interaction of the model with the loading system. This section contains discussions of these sources and indicates errors to be expected from each.

### Model Errors

Torsional rigidity is proportional to the fourth power of cross section dimension. Consequently, slight errors in scaling from prototype to model would be reflected strongly in inaccurate values of  $J_1$ . The likelihood of overall scaling error is small. More likely sources of error would lie in variations of model plate thickness, rib width, rib height and rib spacing as separate entities. All these dimensions are measurable to 0.001 inches directly and may be estimated to 0.0001 with appropriate instrumentation. It was made common practice in the present testing program to measure all dimensions to this latter quantity.

As the result of accidental deviations in the order of 0.0001 in., variations to be expected in  $J_1$  may be evaluated utilizing Eq.(7).

Model material property variations may be considered as negligibly small, since material tests were commonly run on flat plates and repeated on these same plates machined to ribbed plates. In this manner, both absolute values of  $J_1$  and values of  $J_1$  relative to flat plates were obtained.

#### Loading System Errors

As was stated previously, the starting friction in the torque trunnion was maintained below 0.002 in-lbs. Since a typical small load test level was 0.333 in-lbs., the error due to this effect would be 0.6 percent.

Errors in the applied torque could be chargeable to the radius arm and dead weight. As the result of ten measurements of the radius arm, including the half thickness of the loading thread, the arm variations were found to be  $\pm 0.0002$  in. in an average arm length of 2.0175 in. Each load weight variation, determined in a corresponding manner, was found to be  $2 \times 10^{-5}$  lbs. per dead weight of 0.16 lbs.

#### Twist Measuring System Errors

One primary source of error lay in the stability of the electronic circuitry associated with the sensor pairs. The drift amounted to approximately 0.002 radians per hour effective twist deviation. This was determined after a suitable warm-up period.

Since each test was completed within ten minutes, the twist drift would amount to  $3.3 \times 10^{-4}$  radians per test. Calibration before each run provided optimum accuracy during a test.

The reliability of data depended upon the linearity of signal as a function of rotation in each sensor pair. Repeated calibrations established clearly a linear range of 0.1 radians for each pair. In selecting slopes of the plotted data, points well within 3 degrees (or 0.05 radians) were selected to determine m and n.

#### Calibration Procedure Error

Each sensor pair was calibrated by application of a measured vertical motion to a cross arm at the loading head. This rotation was transmitted as a rigid body motion throughout the model. The response of the sensor pair was then plotted as a function of this measured rotation.

The calibration micrometer was marked to indicate directly 0.0005 inches. The arm over which it acted was 4.622 inches. A series of measurements of the calibration arm indicated a possible variation of 0.02 percent in this quantity. In running a test, the screw was always turned in one direction to eliminate backlash.

### Error Due to Interaction of Model with Loading System

The model was loaded and supported by trunnions acting parallel to the twist axis. These trunnions were ground and polished to minimize friction resistance. The effect of frictional resistance would be to generate warping restraint of the model. For thick models this would be a negligible factor since the stiffness of the model could overcome this starting friction.

In thin models (sheet thickness in the 0.040 in. range) this could become a problem. Some of the nonlinearity and scatter in the data obtained with thinner models was charged to this effect. Attempts were made on subsequent tests to avoid thin models in evaluating  $J_1$ .

Another problem with thin models was the effect of sag between supports. This was observed to induce a stiffening action of variable character, and furthermore to give rise to low twist buckling. This effect also was minimized by the use of thicker models (sheet thickness in the 1/8 in. range).

## EXPERIMENTS

### Introduction

Two sets of tests were run in conjunction with the proving of the final design of the torsion testing machine. One group was run on a flat plate, while the other was performed on a ribbed plate. The results of these tests and correlation of the experimental data with theory are reported in this section.

### Typical Test Run

Data for a representative test on a flat plate are shown in Fig. 5, which contains both the calibration and test curves. From these results it is found that

$$m_A = 49.09 \text{ volts/radian}$$

$$m_B = 62.67 \text{ volts/radian}$$

$$n_A = 0.1289 \text{ volts/in-lb.}$$

$$n_B = 0.05403 \text{ volts/in-lb.}$$

$$L = 10 \text{ in.}$$

Therefore,

$$(n/m)_A = 2.626 \times 10^{-3} \text{ radians/in-lb.}; (n/m)_B = 8.621 \times 10^{-4} \text{ radians/in-lb.}$$

and consequently using Eq.(20),

$$GJ_1 = \frac{10 \text{ in.}}{1.764 \times 10^{-3} \text{ radians/in-lb.}}$$

or 
$$GJ_1 = 5.67 \times 10^3 \text{ in}^2 \text{ lb/rad}$$

In order to depict, graphically, the relation between torque and twist, the test data of Fig. 5 were transformed for replotting as shown in Fig. 8. The linearity is evident from the data. A curve for one of the runs on the ribbed plate is also included in Fig. 8.

#### Flat Plate Tests

The flat plate model data are shown in Table 1 together with the theoretical value of  $GJ_1$  computed according to Eq.(7). The average of the five runs made on this specimen differs from the theoretical value by 1.4 percent.

#### Ribbed Plate Tests

Data for the ribbed plate tests are shown in Table 1, from which it may be seen that the average of the three experiments on this model differed from the theoretical  $GJ_1$  by 1.2 percent.

#### Discussion

The agreement of theory and experiment for the two structures tested in connection with this program reveal the reliability

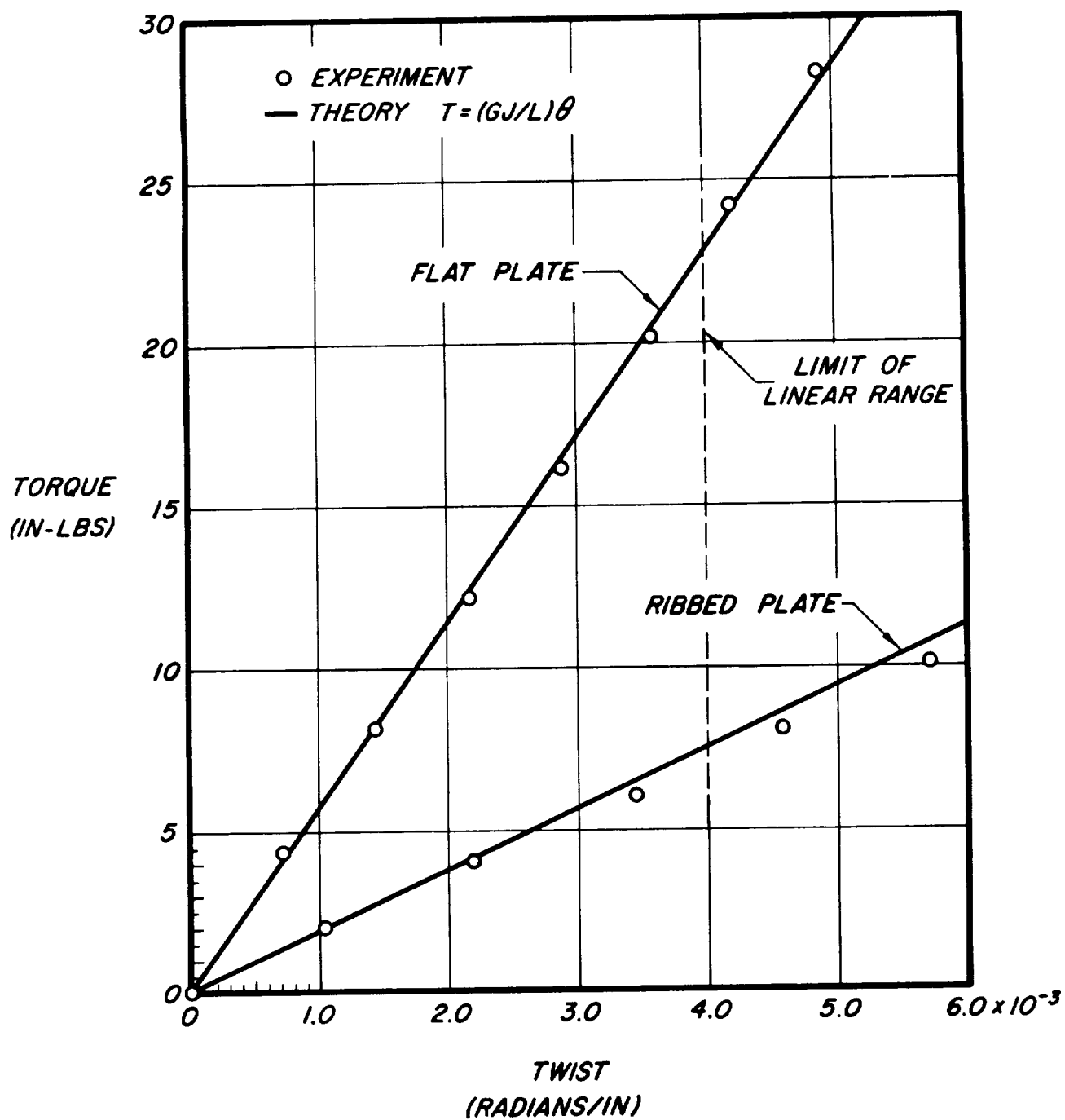
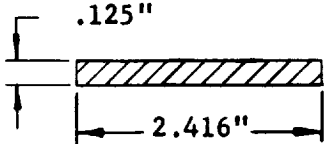
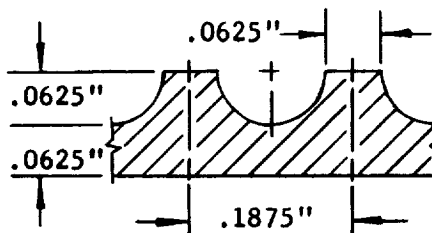


FIGURE 8 TORQUE vs TWIST FOR FLAT AND RIBBED PLATES OF TABLE I. (MEASURED FROM BEGINNING OF LINEAR RANGE OF SYSTEM).

**TABLE 1 - SUMMARY OF EXPERIMENTAL DATA**

| Specimen<br>Description   | Theo.<br>$GJ_i$<br>(in <sup>2</sup> lb/rad) | Run<br>No. | Exp.<br>$GJ_i$<br>(in <sup>2</sup> lb/rad) | $[GJ_{iTh} - GJ_{iExp.}]/GJ_{iTh}$<br>(Percent) |
|---|---|------------|--|---|
|  | $5.70 \times 10^3$                          | 1          | $5.67 \times 10^3$                         | 0.53  |
|   |   | 2          | $5.50 \times 10^3$                         | 3.51  |
|   |   | 3          | $5.65 \times 10^3$                         | 0.88  |
|   |   | 4          | $5.71 \times 10^3$                         | 0.18  |
|   |   | 5          | <u><math>5.59 \times 10^3</math></u>       | <u>1.93</u>                                     |
|   |   | Avg.       | $5.62 \times 10^3$                         | 1.4   |
| Material: 6061-T6 Al for both   |   |            |  |   |

|  |                         |                                    |                               |             |
|--|-------------------------|------------------------------------|-------------------------------|-------------|
|  | 1.888 x 10 <sup>3</sup> | 1                                  | 1.848 x 10 <sup>3</sup>       | 2.12        |
|  |                         | 2                                  | 1.888 x 10 <sup>3</sup>       | 0.00        |
|  |                         | 3                                  | <u>1.863 x 10<sup>3</sup></u> | <u>1.33</u> |
|  |                         | Avg.                               | 1.866 x 10 <sup>3</sup>       | 1.2         |
|  |                         | L = 10", Width = 2.250" (12 ribs). |                               |             |



of the apparatus which was described in the preceding sections. It is now being applied to a variety of structural shapes in connection with a research program on the nature of general instability of stiffened cylinders.

New York University  
October 1961

## REFERENCES

1. Becker, H., "Handbook of Structural Stability, Part VI - Strength of Stiffened Curved Plates and Shells," NACA TN 3786, July 1958.
2. Gerard, G. and Becker, H., "Handbook of Structural Stability, Part VII - Strength of Thin Wing Construction," NASA TN D-162, September 1959.
3. Becker, H. and Gerard, G., "Elastic Stability of Orthotropic Shells," New York University Report SM 60-9, November 1960.
4. Libove, C. and Hubka, R. E., "Elastic Constants for Corrugated-Core Sandwich Plates," NACA TN 2289, February 1951.
5. Dow, N. F., Libove, C. and Hubka, R. E., "Formulas for the Elastic Constants of Plates with Integral Waffle-Like Stiffening," NACA TR 1195, 1954.
6. Crawford, R. F. and Libove, C., "Shearing Effectiveness of Integral Stiffening," NACA TN 3443, June 1955.
7. Hoppmann, W. H., "Bending of Orthogonally Stiffened Plates," J. App. Mech., v. 22, No. 2, June 1955, pp. 267-271.
8. Hoppmann, W. H., Huffington, N. J. and Magness, L. S., "A Study of Orthogonally Stiffened Plates," J. App. Mech., v. 23, No. 3, September 1956, pp. 343-350.
9. Timoshenko, S., "Theory of Elasticity," McGraw-Hill, 1934.
10. Lyse, I. and Johnston, B. G., "Structural Beams in Torsion," Trans. ASCE, v. 101, 1936, pp. 857-896.
11. Trayer, W. and March, H. W., "The Torsion of Members Having Sections Common in Aircraft Construction," NACA TR 334, 1929.
12. Papirno, R., "Elevated Temperature Extensometer Using a Differential Capacitor Sensor," New York University Report No. SM 60-2, January 1960.



